

Clay Mineral Assemblages in Recent Thermal Anomalies of Southern Kamchatka

A.V. Sergeeva✉, D.K. Denisov, M.A. Nazarova

*Institute of Volcanology and Seismology, Far Eastern Branch of the Russian Academy of Sciences,
bul'var Piipa 9, Petropavlovsk-Kamchatsky, 683006, Russia*

Received 23 May 2018; received in revised form 22 October 2018; accepted 8 November 2018

Abstract—We consider the factors determining the mineral composition of hydrothermal clays in recent thermal anomalies of the Pauzhetka–Kambal'nyi–Koshelevskii region and Ebeko (Paramushir Island) and Mutnovskii Volcanoes. The composition of mineral assemblages is influenced by a number of interdependent factors: the type of discharge (steam–gas jets, steaming ground, and mud water pools), temperature, pH, and E_h of a thermal solution. Mineral assemblages including sulfur, opal, α -quartz, and alunite group minerals form on the steaming ground of the craters of active volcanoes (Ebeko and Mutnovskii). Mud water pools of the craters contain mainly sulfur, opal, and α -quartz. An assemblage of kaolinite, opal, alunite group minerals (in small amounts), and goethite forms in mud water pools with pH = 2–3 in the thermal fields of the Pauzhetka–Kambal'nyi–Koshelevskii region. An assemblage of newly formed kaolinite, smectite, pyrite, marcasite, and, sometimes, opal is specific to mud water pools with pH > 3.5–4.0. At pH > 5, smectite, pyrite, and opal are produced. In the thermal fields of the Pauzhetka–Kambal'nyi–Koshelevskii region, the walls of steam–gas jets that are often flooded with water and dry out are formed by kaolinite, smectite, opal, α -quartz, pyrite, marcasite, and goethite. The walls of steam–gas jets that are not flooded with water for a long time consist of kaolinite, opal, α -quartz, smectite (traces), alunite group minerals, pyrite, and marcasite in close amounts. The steaming ground of the thermal fields of the Pauzhetka–Kambal'nyi–Koshelevskii region is composed of kaolinite, alunite group minerals, opal, and goethite or an assemblage of kaolinite, smectite, opal, pyrite, and marcasite.

Keywords: thermal fields, hydrothermal clays, montmorillonite, kaolinite, alunite group minerals

INTRODUCTION

Hydrothermal clays and argillized rocks forming in recent thermal fields of southern Kamchatka are interesting in many aspects. They are investigated in the context of mineral formation for solving engineering geology problems (Martinez et al., 2006; Frolova et al., 2016), as part of hydrothermal systems (Rychagov, 2014; Rychagov et al., 2017a,b,c), and as barriers for elements transferred by a hydrothermal flow (Rychagov et al., 2010).

Clay minerals are examined as indicators of their formation conditions (Drits et al., 2011; Ogorodova et al., 2013; Krupskaya et al., 2017). Study of the mineral composition of hydrothermal clays formed in recent thermal fields of Iceland (Geptner et al., 2007) showed that kaolinite and smectite are the most common clay minerals at fumarole sites. Clay minerals that formed in recent hydrothermal systems are a finely dispersed and structurally disordered material (Eroshchev-Shak et al., 2005). Drilling of hydrothermal clay sheets in thermal anomalies showed a gradual change of chlorite–smectite assemblage by kaolinite–smectite one with depth (Miyoshi et al., 2015).

Volcanic rocks transform into argillized ones upon their contact with a hydrothermal flow. The hydrothermal activity leads to the transformation of glass of igneous rocks into clay minerals; pyroxenes are more seldom transformed (Ladugin et al., 2014; Frolova et al., 2016). Therefore, clay strata form at the exits of thermal fluids and then play a special role in the structure of the hydrothermal system. They actively interact with a hydrothermal flow and transform; the transformation products are determined by both the composition of the contacting solution and its temperature.

Study of the key sections (Rychagov et al., 2008) showed that hydrothermal clays are locally heterogeneous on a scale of 100–1 cm, which is expressed as a significant spatial variation in mineral and elemental compositions both in the normal and in the tangential directions relative to the day surface (Kravchenko and Rychagov, 2017; Rychagov et al., 2017a,b,c). Anomalies and a wide scatter in contents of Au, Ag, Pb, As, Hg, etc. were revealed (Rychagov et al., 2002). Research into the behavior of mercury in hydrothermal systems showed that its content varies and depends on the type of thermal effect, the mineral composition of the sample, and the type of deposit (Rychagov, 2009b; Rychagov et al., 2009a,b, 2012a, 2014). A relationship between the mineral composition and the local geochemical conditions was established in study of the microheterogeneity of dioctahedral

✉ Corresponding author.

E-mail address: valraf2009@yandex.ru (A.V. Sergeeva)

mica minerals (Drits et al., 2013). The authors think that this microheterogeneity is the result of the local difference in geochemical environments during the mineral formation. The microtexture of hydrothermal clays was also studied in the context of their interaction with a thermal flow (Rychagov et al., 2010, 2012b).

Local fluctuations in geochemical conditions in thermal fields are determined by the type of discharge. Recent thermal fields are a natural test ground for monitoring the formation and transformation of clay minerals. Owing to high temperatures (up to 100 °C) and the presence of a liquid component, the rates of mineral formation and transformation are rather high.

There are several types of discharge in the recent thermal fields of the Pauzhetka–Kambal’nyi–Koshelevskii district, which differ in the water regime and, hence, in the mineral composition of clays (Figs. 1 and 2):

(1) Mud and mud water pools. A common feature of all pools is the contact of a heated steam–gas jet with a water–clay suspension. The temperature in mud water pools is about 100 °C and can stay constant for a long time, pH is 2–7, and E_h is usually positive (oxidizing conditions). Thermal lakes have a temperature mainly below 100 °C; as for the rest, they can be considered a kind of mud water pools.

(2) Steam–gas jets. They are a steam flow exiting to the day surface along a well-defined channel. When the flow exits, its temperature decreases to 100 °C, but the exit temperature of powerful high-temperature jets can be higher. Most often, a steam–gas jet generates a hollow periodically

flooded with meteoric waters and turns into a mud water pool. When drying out, this pool again functions as a steam–gas jet.

(3) Steaming ground. It has a temperature of about 100 °C or lower, lack a well-defined channel for fluid exit, and is relatively dry. At active sites of thermal anomalies, the temperature of steaming ground can be higher than 100 °C. Such sites form when a fluid flow is reduced; the heat carrier moves to the surface mainly along small fractures in the clayey ground. A specific feature of steaming ground is crystallization of salts at the surface, which proves the relatively quiet infiltration of a hydrothermal fluid (Zhitova et al., 2017).

We have studied samples taken in the Lower Koshelevskii, Upper Koshelevskii, South Kambal’nyi Far, and South Kambal’nyi Central thermal anomalies, North Kambal’nyi steam jets, and East Pauzhetka and Upper Pauzhetka thermal fields. Pools with pH close to the neutral value are present in the Lower Koshelevskii thermal anomaly, and more acidic solutions occur in the Upper Koshelevskii and South Kambal’nyi Far thermal fields. We have also examined samples from the thermal anomalies of the active Ebeko (Paramushir Island) and Mutnovskii Volcanoes.

The aim of this research was to study the mineral (phase) composition of hydrothermal clays formed during the discharge of hydrotherms of different types and with different values of physicochemical parameters (temperature and composition) and to determine the specific features of thermal manifestations of each type.

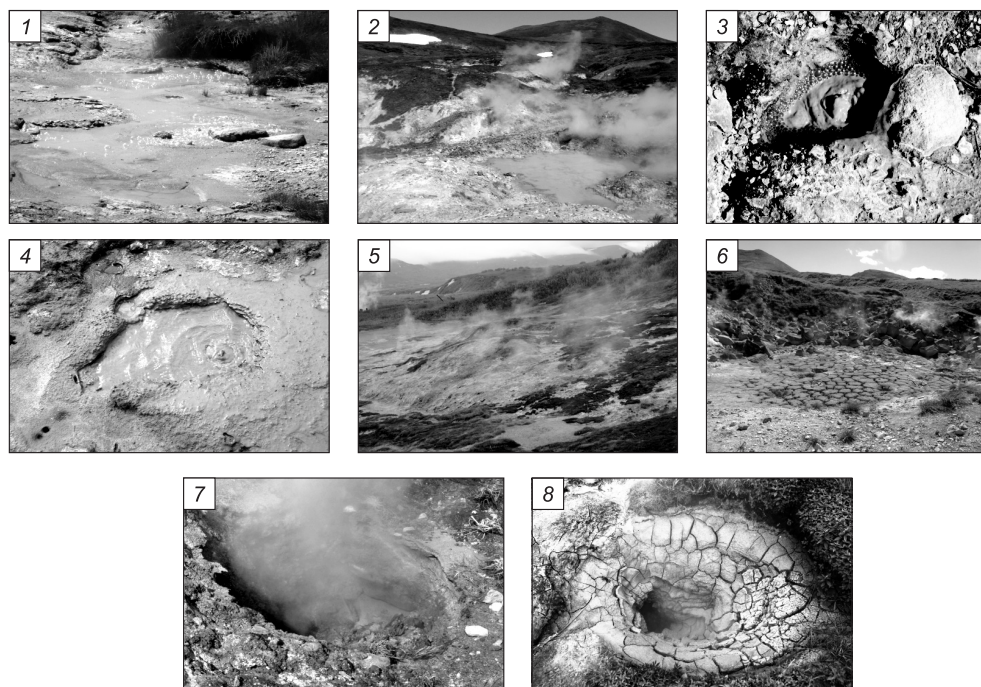


Fig. 1. Diverse thermal manifestations of the Pauzhetka–Kambal’nyi–Koshelevskii region; thermal lakes (1, 2), mud water pools (3, 4), steaming ground (5, 6), and steam–gas jets (7, 8) localized in the North Kambal’nyi steam jets (1, 3), Upper Koshelevskii thermal anomaly (2), Upper Pauzhetka thermal fields (4, 5, 8), and Lower Koshelevskii thermal anomaly (6, 7).

		Active crater (Ebeko and Mutnovskii Volcanoes)		Thermal anomalies of the Pauzhetka–Kambal’nyi–Koshelevskii region				
				Mud water pool, pH			Heated ground	Steam–gas jet
				2–3	3–4	4–7		
		Mud water pool	Heated ground					
Opal, quartz		■		■	■	■	■	■
Sulfur		■		■	■			■
Alunite group minerals	Natro- alunite	■		■	■	■	■	■
	Ammonio- jarosite			■	■	■	■	■
Newly formed kaolinite				■	■	■	■	■
Crystallized kaolinite						■	■	■
Montmorillonite					■	■	■	■
Pyrite					■	■	■	■
Marcasite					■	■	■	■
Goethite				■	■	■	■	■
Soluble sulfates and alum			■			■	■	■

Fig. 2. Scheme of the mineral composition of clays of different thermal manifestations: persistent and predominant minerals (1), minor minerals (2), and rare minerals (3). Free cells mean the absence of the minerals.

GEOLOGIC AND GEOTHERMAL CHARACTERISTICS OF THE OBJECTS OF STUDY

The research was carried out in the recent hydrothermal systems of the Kuril–Kamchatka region. Most of the samples were taken in the Pauzhetka–Kambal’nyi–Koshelevskii geothermal (ore) region of southern Kamchatka (Fig. 3). The area is a long-living (from Oligocene to Holocene) volcanic ore center (Vasilevskii, 1977). It comprises three large geologic and hydrogeologic structures: Pauzhetka hydrothermal system, the Kambal’nyi Volcanic Ridge, and the Koshelevskii volcanic massif (Masurenkov, 1980). The recent (Holocene) stage of their evolution is marked by the formation of thermal anomalies, namely, steam–hydrotherm discharge zones. Thermal anomalies are one or several thermal fields localized in certain geologic structures: elevated tectonic (tectonomagmatic) blocks, apical parts of subvolcanic intrusions, fracturing zones above deep faults, erosion craters of ancient volcanoes, etc. (Belousov and Lomonosov, 1993; Feofilaktov et al., 2017). Geothermal heat, steam–gas mixture, and hydrothermal solutions discharge as ground steaming, steam–gas jets, water and mud water pools, and pulsating and other gushing water springs (Fig. 1). The temperatures of grounds, steam–gas jets, and springs reach 98–

105 °C (in the thermal fields of the Pauzhetka system and the Kambal’nyi Ridge) and 120–150 °C (in the thermal anomalies of the Koshelevskii massif). In the zone of hydrotherm discharge (on the day surface), weakly acidic to neutral sulfate ammonium waters with a complex cationic composition and an average mineralization of 0.5–1.0 g/L are predominant (Kalacheva et al., 2016).

Material for comparison of mineral assemblages was also obtained in the Donnoe thermal field of the Mutnovskii Volcano (southern Kamchatka) and in the Northeastern fumarole field of the Ebeko Volcano (Paramushir Island) (Fig. 3). Both volcanoes are active. The temperatures of steam–gas jets (fumarole) in the periods of volcanic activity can exceed 500 °C (Kotenko et al., 2012). Sampling was made during the stationary (normal) gas–hydrothermal activity of the volcanoes, when the temperatures of grounds and steam–gas jets were no higher than 100–105 °C. The water in the zone of hydrotherm discharge is acidic and ultra-acidic. The map of the area and the location of the thermal fields are presented in Fig. 3.

The volcanic rocks of the Pauzhetka–Kambal’nyi–Koshelevskii region are composed mainly of basaltic andesites, basalts, olivine–pyroxene basalts, and dolerite-basalts (Pozdeev and Nazhalova, 2008). The rocks of all studied objects

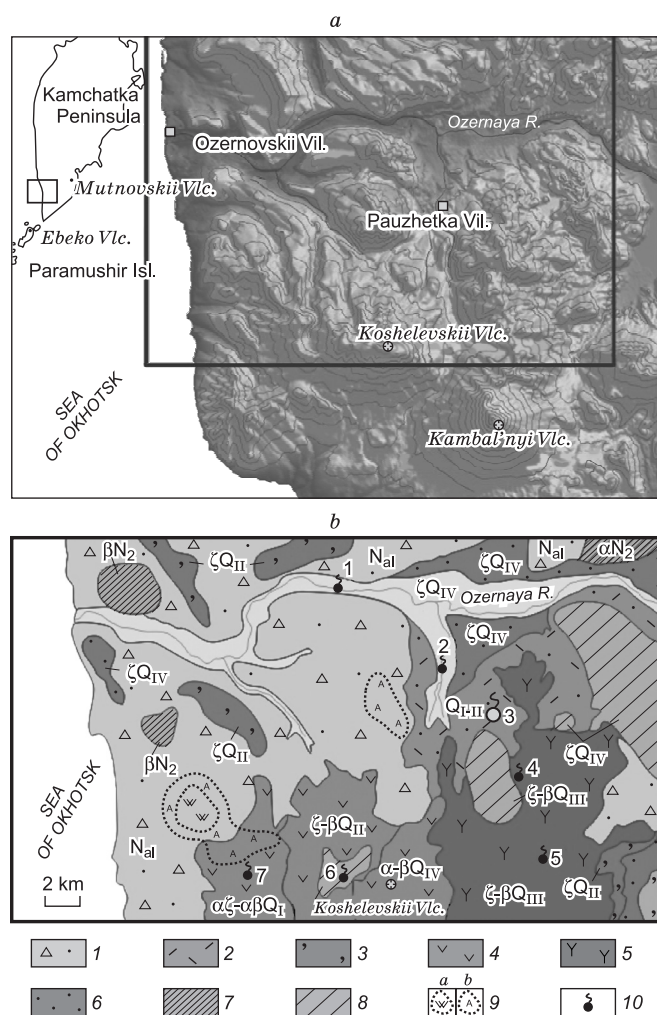


Fig. 3. Geographical (a) and geological (b) maps of the southwestern part of the Kamchatka Peninsula. 1, Neogene lava-pyroclastic deposits; 2, volcanosedimentary deposits (tuffs) of the Pauzhetka Formation; 3, ignimbrites (dacites and rhyodacites), 4, lava complex of the Koshchelevskii volcanic massif; 5, volcanic rocks (lavas, pyroclastic flows, and extrusions) of the Kambal'nyi Ridge; 6, dacites (pumice deposits); 7, subvolcanic and extrusive bodies of basalts and andesites; 8, extrusive subvolcanic bodies of contrasting composition; 9, hydrothermally altered rocks, a, secondary quartzites, b, argillizites; 10, geothermal fields: 1, first hot springs, 2, Pauzhetka hydrothermal deposit, 3, North Kambal'nyi steam jets, 4, Central Kambal'nyi, 5, South Kambal'nyi, 6, Upper Koshchelevskii, 7, Lower Koshchelevskii (Rychagov et al., 2014; Zhitova et al., 2017, 2018).

have some compositional similarities. The Ebeko Volcano is formed by andesites and andesitic basalts, whereas its base is composed of highly altered volcanic rocks (Late Pleistocene). The Mutnovskii volcanic edifice comprises four merged cones of a stratovolcano with peak calderas and daughter intracaldera edifices and is formed by rocks from basalts to rhyodacites. High-alumina basalts are predominant, but the tephra of the youngest crater (Active funnel) is composed of high-alumina K–Na basaltic andesites (Chashchin et al., 2011; Frolova et al., 2016).

METHODS

Clays were sampled from the surface and throughout the depth of mud pools, because clay suspension is continuously mixed as a result of bubbling. At the sites with heated ground, a layer-by-layer pit sampling was performed. During a gradual excavation of steam–gas jets, samples were taken from the jet walls being in contact with steam.

During the sampling, pH, E_h , and T of the samples were measured. The former two parameters were measured with portable pH and E_h meters (Hanna Instruments, HI 98121, and HI 98129) with an accuracy of ± 0.05 (pH) and ± 2 mV (E_h). The temperature was evaluated with temperature gauges (thermocouples and thermal resistances). The values of pH and E_h were determined for mud and mud water pools, and temperature was measured in all cases.

Multiphase samples were separated into clay, heavy, and light fractions by standard procedures, annealed to an air-dried basis, converted to monoionic forms, and again annealed. The separated fractions were studied by X-ray diffraction and IR spectroscopy.

Diffraction patterns were recorded on an XRD 7000 X-ray (Shimadzu) diffractometer in the range $4\text{--}60^\circ 2\theta$, with a step of $0.05^\circ 2\theta$ and in the continuous-scanning mode with a speed of 0.5 deg/min , which is equivalent to a 6 s exposure at the point. Samples containing smectite were examined in the air-dried and glycerin-saturated states.

Infrared spectra were recorded using an IR Affinity Fourier IR spectrophotometer (wavenumber $400\text{--}4000 \text{ cm}^{-1}$, resolution $2\text{--}4 \text{ cm}^{-1}$, $60\text{--}80$ scans). The air-dried samples were ground with KBr in an agate mortar and pressed into tablets.

Clay minerals were identified from the data of detailed X-ray diffraction and IR spectroscopy. To determine the type of substitution in smectite, a Green–Kelly test of some samples was made. Smectite of the samples was converted into a Li-saturated form and then was annealed at 250°C for 6 h. In the course of the test, the smectite lost its capability to expand during glycerol intercalation, which indicates that the charge is concentrated mostly in the octahedral layer (Chukhrov, 1992).

Kaolinite was identified by X-ray diffraction and IR spectroscopy. In the diffraction patterns, kaolinite had a basal reflection peak near $d(001) = 7.1 \text{ \AA}$. In the IR spectra, kaolinite was identified from a series of intense bands that are absent for montmorillonite. The main difference between these minerals was observed in the high-frequency region, where the bands of stretching vibrations of water and OH groups are present. The spectrum of kaolinite has a sharp peak at $\sim 3700 \text{ cm}^{-1}$ and a slightly less intense but narrow peak at $\sim 3625 \text{ cm}^{-1}$ (Chukhrov, 1992).

The interplanar spacing $d(001)$ in air-dried smectite varies from 14.3 to 15.5 \AA , and in the case of glycerol intercalation it increases to $18.0\text{--}18.5 \text{ \AA}$. These parameters correspond to smectite with calcium in the interplanar space

Table 1. Phase composition of mineral mixtures formed in thermal fields

Discharge	Mineral composition of mixture
Heated grounds of active craters, after contact with ultra-acidic solutions	Sulfur, opal, α -quartz, alunite group minerals, soluble sulfates
Mud water pool of active crater	Sulfur, opal, α -quartz
Mud water pool with pH = 2–3	Kaolinite, opal, alunite group minerals (minor), goethite
Mud water pool with pH > 3–4	Kaolinite, smectite, pyrite, marcasite, opal (occasional), goethite, alunite group minerals
Mud water pool with pH ~ 5	Smectite, pyrite, opal, calcite (occasional), goethite
Steam–gas jets often flooded with water and drying out	Kaolinite, smectite, opal, quartz, pyrite, marcasite, goethite
Steam–gas jets not flooded with water for a long time	Kaolinite, opal, quartz, smectite (traces), alunite group minerals, pyrite and marcasite in close amounts
Heated grounds	Kaolinite, alunite group minerals, opal, goethite, smectite (traces)
Heated grounds	Kaolinite, smectite, opal, pyrite, marcasite

(Chukhrov, 1992). The Green–Kelly test of several smectite samples showed substitution of the predominantly octahedral layer, and the IR spectra revealed major substitution of Al by Fe^{3+} and Mg (shoulders at ~ 840 and 880 cm^{-1}), which gives grounds to assign the smectite to montmorillonite (Madejova and Komadel, 2001; Madejova, 2003).

Identification of opal and α -quartz. Opal is recognized in diffraction patterns from a noticeable halo in the range $15\text{--}30^\circ 2\theta$ (Fig. 4), and in the IR spectra it is determined from broad peaks at 1100 , 800 , and 470 cm^{-1} . Minerals of the alunite group were identified from X-ray diffraction and IR spectroscopy data. The most obvious differences between the samples of different compositions are observed in the region of stretching vibrations of OH groups. Natroalunite is identified from the characteristic absorption bands at 3460 and 3485 cm^{-1} and less intense bands at 600 , 630 , and 685 cm^{-1} . Ammoniojarosite is recognized from the intense band at 3416 cm^{-1} ; minamite-2R, from bands at 3486 and 3510 cm^{-1} ; and ammonioalunite, from a band at 3514 cm^{-1} (Pamela et al., 2009). Ammonium minerals of the alunite group show a band at 1430 cm^{-1} ($\nu_4(\text{NH}_4^+)$).

DISCUSSION

The temperatures of the studied sites of steaming ground are within $50\text{--}105 \text{ }^\circ\text{C}$, and the temperatures of steam–gas jets are higher, $100\text{--}140 \text{ }^\circ\text{C}$, but mostly about $100 \text{ }^\circ\text{C}$. The investigated mud and mud water pools are characterized by temperatures of $95\text{--}100 \text{ }^\circ\text{C}$ and pH from 0 (thermal fields of the craters of the active Ebeko and Mutnovskii Volcanoes) to 7–8 (hydrotherm discharges of the Lower Koshelevskii thermal anomaly). The redox potential (E_h) shows significant variations, from -240 mV (reducing conditions) to $+300 \text{ mV}$ (oxidizing conditions). The correlation between pH and E_h is weak, because the processes controlling pH and the potential-determining reactions are often different; E_h has a significant influence on the composition of the ore fraction. In addition to clay minerals, there is a wide range of other minerals in the thermal fields: gypsum, barite, cal-

cite, including magnesian one, aragonite, apatite, zeolites (mordenite, heulandite, laumontite, and stilbite), variscite, metavariscite, binary sulfides (pyrite, marcasite, cinnabar, etc.), ternary sulfides (chalcopyrite), etc. There are also soluble salts crystallizing at the surface of clay blankets. These are mainly alum group minerals and crystallohydrates of aluminum and iron sulfates; also, rare minerals of the voltaite group and other minerals occur. Here we consider only the minerals that quantitatively dominate over others.

The most typical mineral assemblages of the studied thermal anomalies are presented in Table 1 and, schematically, in Fig. 2.

Almost all the mixtures include the most stable minerals of the initial rocks: feldspars (sanidine, anorthoclase, and plagioclases), pyroxenes (similar in composition to enstatite and hypersthene or augite), and amphiboles similar to hornblende.

Mineral assemblages of steaming ground and mud water pools of active craters. The mud pools of the craters of the active Ebeko (Paramushir Island) and Mutnovskii Volcanoes are characterized by pH ~ 0 and a temperature of $100 \text{ }^\circ\text{C}$. They contain mineral assemblages formed under the

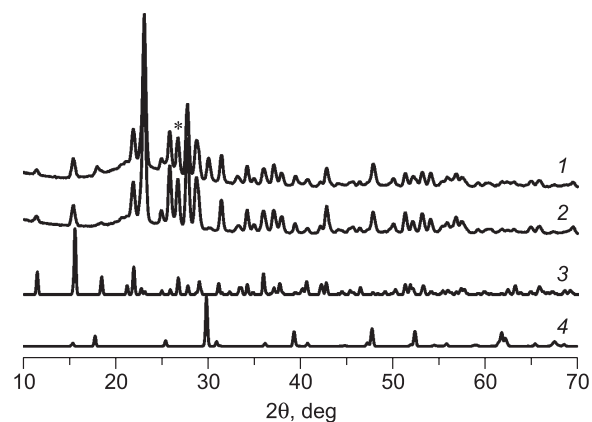


Fig. 4. Diffraction patterns of clay suspensions from mud water pools of the craters of the Ebeko (1) and Mutnovskii (2) Volcanoes, theoretical diffraction patterns of sulfur (3) and natroalunite (4). Asterisk marks the superposition of the reflex of α -quartz.

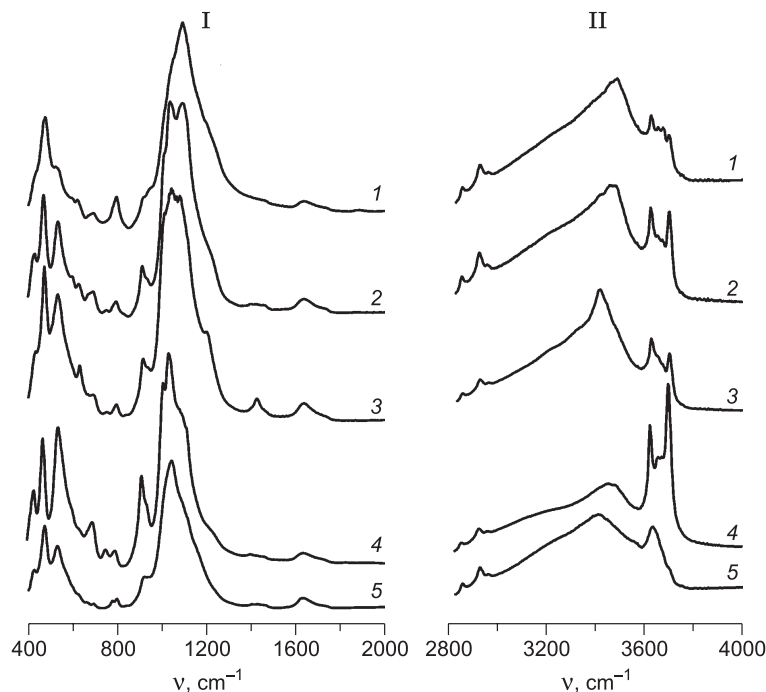


Fig. 5. IR spectra of the clay fractions of mud water pools with pH = 1.5–3.0 (1, 2, 3) and 4–6 (4, 5), sampled from the South Kambal'nyi Far (2, 5) and Upper Koshelevskii thermal field (1, 3, 4). I, range 400–2000 cm^{-1} , II, range 2800–4000 cm^{-1} .

action of ultra-acidic solutions. The clay suspension in the pools and the steaming ground consist of opal, alunite group minerals, and sulfur (Fig. 4). The dry heated sites of the grounds have a higher content of alunite than the suspension in the pools, but the qualitative mineral composition is the same. The heavy (ore) fraction is negligible. Often, there are gypsum and coatings of soluble sulfates at the surface of steaming ground.

Mineral assemblages of this composition formed upon the contact with acidic solutions at high fumarole activity (Mutnovskii and Ebeko Volcanoes). Both volcanoes have fumaroles, whose mouths are framed with sulfur; the fumarole gases are rich in SO_2 .

Mineral assemblages of the thermal fields of the Puzhetka–Kambal'nyi–Koshelevskii region. The thermal fields have more diverse conditions: There are mud water pools with pH = 1.5–6.0, grounds heated to 100–112 °C, and steam–gas jets of different power.

Mineral assemblages of mud water pools of thermal anomalies. Figure 5 shows the IR spectra of clays formed in the mud water pools with pH = 1.5–6.0. The spectra have distinct bands in the ranges 400–600, 1000–1100, and 2800–3700 cm^{-1} , specific to layered silicates. In the region 400–600 cm^{-1} , there are two intense bands with peaks near 470 and 540 cm^{-1} ; the other bands are less intense. The assignment of the absorption bands is given in Table 2.

The mud pools with pH ≤ 3 contain an assemblage of opal and newly formed kaolinite; alunite group minerals and goethite are minor, and smectite is absent. The curves in Fig. 5 mark a predominance of certain minerals in the clay

Table 2. Absorption bands of layered silicates

Band, cm^{-1}	Assignment
430	$\nu_2(\text{Si-O})$
470	$\delta(\text{Si-O-Si})$
530	$\delta(\text{Me}^{\text{VI}}\text{-O-Si})$
580	$\gamma(\text{OH})$, alunite group minerals
630	$\nu_4(\text{Si-O})$, smectite
695	$\nu_4(\text{Si-O})$
750	$\nu_4(\text{Si-O})$, kaolinite
795	$\nu_1(\text{Si-O})$, α -quartz $\delta(\text{Mg-O(H)-Fe}^{3+})$
840	$\delta(\text{Al-O(H)-Mg})$
880	$\delta(\text{Al-O(H)-Fe}^{3+})$
915	$\delta(\text{Al-O(H)-Al})$
935	$\delta(\text{Al-O(H)-Al})$
1010	$\nu_1(\text{Si-O})$
1035	$\nu_3(\text{Si-O})$
1110	$\nu_3(\text{Si-O})$
1640	$\delta(\text{H}_2\text{O})$
3220	Overtone $\delta(\text{H}_2\text{O})$ a/or $\nu_3(\text{H}_2\text{O})$ Me(H_2O)
3420	$\nu_1(\text{H}_2\text{O})$ Me(H_2O),
3625	$\nu(\text{OH})$ (hydrogen-bonded); $\nu_3(\text{adsorbed H}_2\text{O})$
3650	$\nu(\text{OH})$
3675	$\nu(\text{OH})$
3700	$\nu(\text{OH})$

fractions: 1—opal, 2 and 4—newly formed aolinite, and 3—ammoniojarosite.

As pH increases to ~3–4, smectite appears in the mixture, and marcasite and pyrite appear in the ore fraction. The mud pools with pH ~ 3.5 have significant amounts of marcasite; as pH slightly increases, marcasite disappears from the ore fraction, and pyrite prevails. Goethite, alunite group minerals, opal, and quartz can be present in small amounts.

In mud pools with pH close to the neutral value, kaolinite virtually does not form or is present in insignificant amounts; smectite forms instead of it. Opal and goethite are minor. Pyrite is predominant in the ore fraction, whereas marcasite is absent.

The diffraction patterns of the clay fractions of the mud water pools are shown in Fig. 6. The broad reflexes indicate a low structural perfection of newly formed phyllosilicates. The octahedral layer in smectite is partly substituted by iron and magnesium ($\text{Fe}_{\text{Al}}^{3+}$, Mg_{Al}), and calcium and sodium are localized in the interplanar space. The thermal solutions of the pools show the following relationships among the concentrations of components: $C(\text{K}^+) \leq C(\text{Mg}^{2+}) < C(\text{Ca}^{2+}) \sim C(\text{Na}^+)$. The concentrations of these elements as well as aluminum and iron are within 10^{-5} – 10^{-3} mole/L. The concentrations of cations in the pore solutions are 4–5 orders of

magnitude higher. Thus, the composition of montmorillonite is in correlation with the composition of the thermal solutions.

Mineral assemblages of steam–gas jets. After the drying-out of mud water pools, clays continue to warm up by a steam flow; at the same time, infiltration of the pore solutions to the walls of the jet channel takes place. This leads to the transformation of the mineral composition of clays: The content of smectite decreases, whereas the contents of kaolinite and alunite group minerals increase. Marcasite–pyrite, opal, alunite, ammoniojarosite–goethite, and other mineral crusts often form on rock fragments localized on the walls of the steam jet channel (Fig. 7).

Clays of steam–gas jets differ from clays of mud pools in a significant portion of marcasite in the heavy fraction (Fig. 8). Feldspar and quartz are predominant in the light fraction. Clays forming the walls of steam–gas jets have a higher content of newly formed, poorly crystallized kaolinite, whereas the content of smectite decreases. A steam–gas jet is often (several times per season) flooded with meteoric waters and dries out, whereas its channels are usually composed of newly formed kaolinite and smectite in commensurate amounts and the heavy fraction is predominantly pyrite and marcasite.

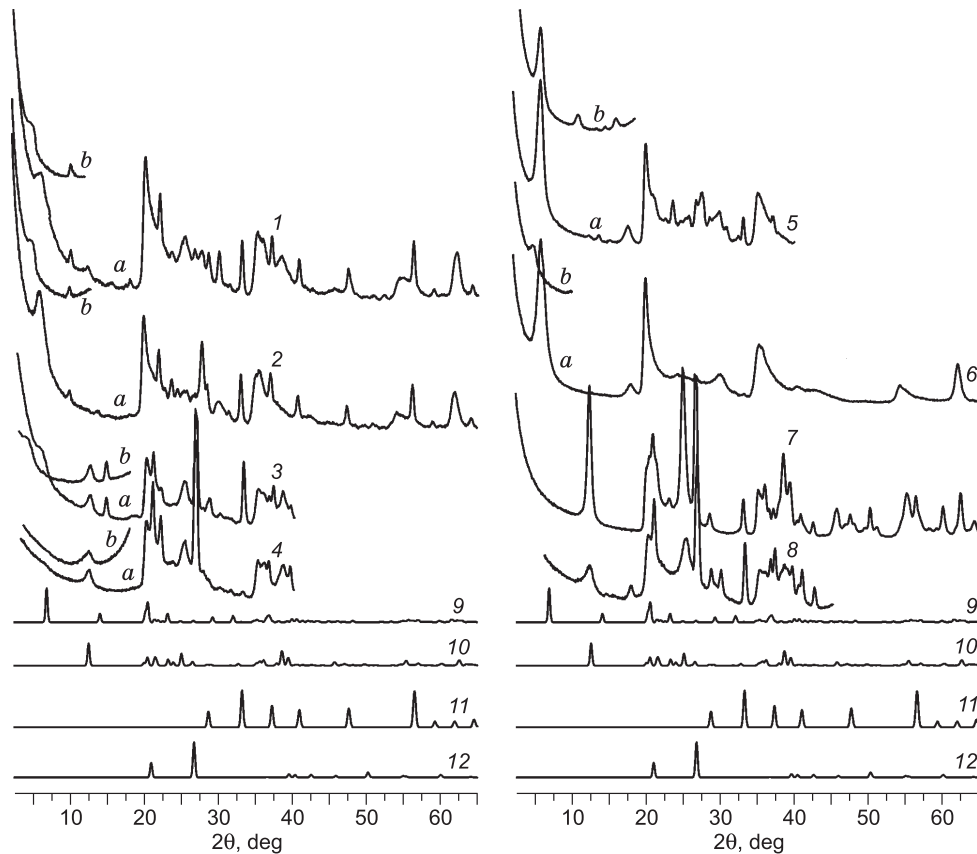


Fig. 6. Diffraction patterns of the air-dried (a) and glycerol-saturated (b) clay fractions of mud water pools (1–4) and steaming ground (5–8) of the Upper Pauzhetka (1, 6), Nizhnii Koshelevskii (2, 3), and East Pauzhetka (5, 7, 8) thermal fields; theoretical diffraction patterns of montmorillonite (9), kaolinite (10), pyrite (11), and α -quartz (12).

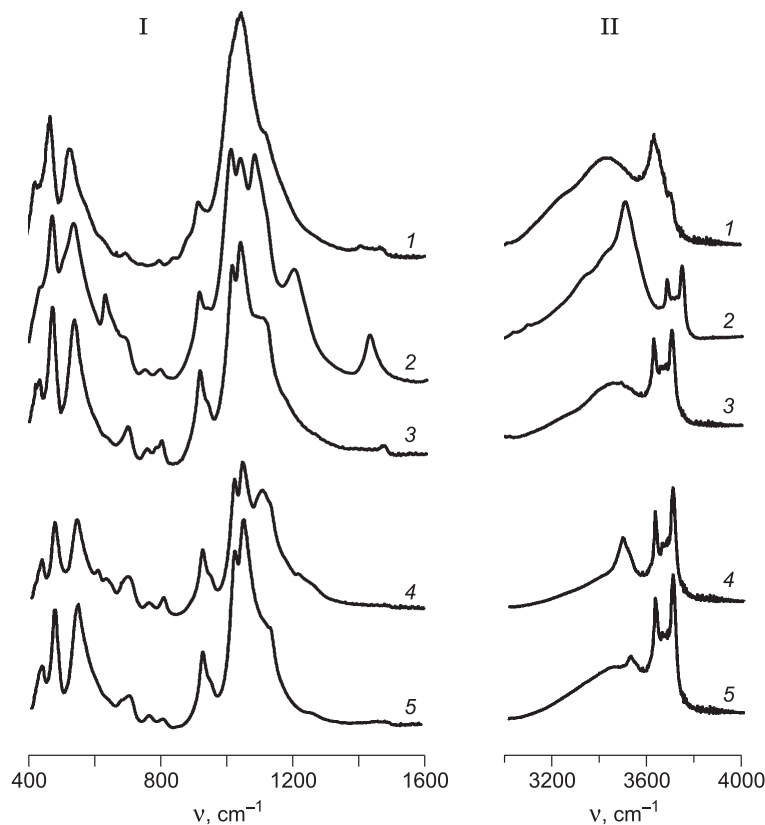


Fig. 7. IR spectra of clays composing the walls of steam–gas jets of the East Pauzhetka thermal field (1, 2), North Kambal’nyi steam jets (3), and Lower Koshelevskii thermal anomaly (4, 5), in the ranges 400–1600 cm^{-1} (I) and 3000–4000 cm^{-1} (II).

If the jet functions in its regime for a long time, then kaolinite with a perfect structure prevails in the clay fraction, marcasite and pyrite are present in close amounts (sometimes, marcasite dominates over pyrite), and also goethite occurs. Minerals of the alunite group are more diverse: Besides ammoniojarosite, there are natroalunite, ammonioalunite, minamiite, natrojarosite, and jarosite. Ammoniojarosite often occurs on the shores of mud pools. It seems to result from the oxidation of marcasite and pyrite, caused by an increase in E_h and a change of the reducing environment by the oxidizing one. The crystallization of alunite group minerals (minamiite, natroalunite, ammonioalunite, and alunite) proceeds more slowly, because it requires a certain concentration of aluminum in the pore solution of clays composing the steam–gas jet channel. Other ions necessary for crystallization of alunite group minerals are present in the pore solutions in high concentrations: $C(\text{Na}^+)$, $C(\text{Ca}^{2+})$, $C(\text{SO}_4^{2-}) \sim 10^{-4}$ – 10^{-1} mole/L, whereas $C(\text{Al}^{3+}) \sim 10^{-5}$ – 10^{-4} mole/L. The steam–gas jet channel serves as an evaporative barrier for the pore solutions; as a result, the concentrations of components locally increase, which leads to the crystallization of natroalunite and minamiite.

As the activity of thermal fields increases, sulfur appears in steam–gas jets (spatial group *Fddd*). In this case, the mineral assemblage of clays is similar to that of active craters: sulfur, opal, α -quartz, and alunite group minerals.

Mineral assemblages of steaming ground. Minerals of dry steaming ground are dominated by kaolinite of different structural perfection but generally better crystallized than kaolinite in mud water pools and steam–gas jets or by opal and alunite group minerals. The latter minerals usually form in the subsurface zone of steaming ground, where they are present in significant amounts. These are mostly natroalunite, minamiite (natroalunite-2R), ammoniojarosite, and ammonioalunite. A distinctive feature of steaming ground is a coating of readily soluble salts, usually sulfates (Zhitova et al., 2017).

Steaming ground composed mainly of alunite group minerals and opal often contains traces of goethite, whereas other minerals of the heavy fraction are absent. When the heated ground consists mostly of kaolinite, the heavy fraction has a significant amount of goethite; also, marcasite in a varying amount and traces of pyrite can be present.

Smectite is rare in steaming ground. It is found only at the sites that are periodically highly moistened, but montmorillonite can be present in significant amounts at a shallow depth (≤ 0.5 m) of such sites. In this case, it is in assemblage with newly formed kaolinite, and the mixture has a composition transitional from mud water pool to heated-ground mineral assemblages. Therefore, steaming ground is generally composed of the following mineral assemblages:

opal + alunite group minerals + kaolinite + goethite and kaolinite + smectite + pyrite ± marcasite.

The cause of the disappearance of montmorillonite from the subsurface zone of the clay strata is the more acidic pore solutions, which is due to:

- oxidation of sulfur-containing compounds;
- concentration of the pore solutions as a result of water evaporation, hydrolysis of iron and aluminum salts, and, as a consequence, acidification of the solutions;
- formation of alunite group minerals, e.g., following the equilibrium $2\text{Na}^+ + 6\text{Al}^{3+} + 10\text{SO}_4^{2-} = 2\text{NaAl}_3(\text{SO}_4)_2(\text{OH})_6 + 6\text{H}_2\text{SO}_4$.

Alunite group minerals crystallize from an aqueous solution, with a gradual shift of the solution composition toward an increase in the content of sulfuric acid. Therefore, when a thermal fluid that arrived directly at the surface of a clay blanket evaporates, it leaves a coating of soluble sulfates and leads to the dissolution of montmorillonite. Dissolution of montmorillonite provides the solution with aluminum, magnesium, and iron, which can form complex sulfates, such as ammoniovoltaite $(\text{NH}_4)_2\text{Fe}_5^{2+}\text{Fe}_3^{3+}\text{Al}(\text{SO}_4)_{12}(\text{H}_2\text{O})_{18}$ (Zhitova et al., 2017, 2018) and minerals of its group.

Marcasite crystallizes on the walls of steam–gas jets and mud pools with pH ~ 3.5; at higher pH, pyrite crystallizes. We can explain this phenomenon by invoking data on the hydrothermal synthesis of marcasite (Murowchick and Barnes, 1986). Polysulfides H_2S_n and their deprotonated forms HS_n^- play a crucial role in the formation of iron disulfides under hydrothermal conditions. A predominance of the deprotonated form HS_n^- leads to the crystallization of pyrite, whereas a predominance of H_2S_n is favorable for the crystallization of marcasite. The undissociated forms H_2S_n begin to dominate at $\text{pH} < \text{p}K_1$, where K_1 is the constant of the first-stage dissociation. The $\text{p}K_1$ values for $n = 2-5$ are in the range 5.0–3.5; therefore, in acidic solutions, under high sulfur activity, marcasite is a major crystallizing mineral. During the experimental hydrothermal synthesis of marcasite (Murowchick and Barnes, 1986), significant amounts of the mineral formed in the pH range 3.4–4.19, whereas at higher pH, mainly pyrite formed. This is, most likely, the cause of the high content of marcasite in acidic solutions and on the walls of steam–gas jets.

CONCLUSIONS

Under fumarole activity in the craters of active volcanoes, acidic thermal solutions (pH ~ 0) favor the formation of an assemblage of quartz, opal, alunite group minerals, and sulfur. At heated dry sites, the content of alunite group minerals is higher than it is in suspension of a mud water pool. Clays of active craters lack a heavy (ore) fraction, except for pyroxene traces.

In the thermal fields of the Puzhetka–Kambal’nyi–Koshelevskii region, the environment continuously changes for a short (on the geologic scale) time. Correspondingly, the

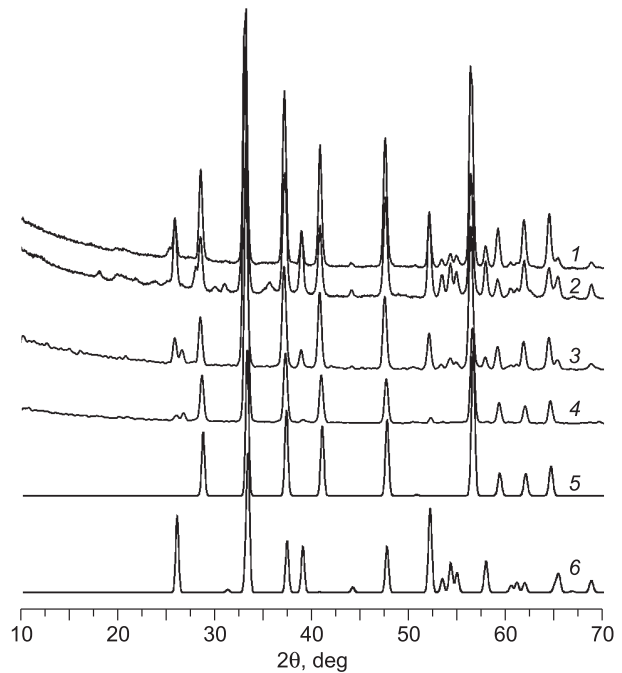


Fig. 8. Diffraction patterns of the ore fractions of clays of mud water pools with pH = 3 (1) and 6 (2) and steam–gas jets (3, 4) and theoretical diffraction patterns of pyrite (5) and marcasite (6).

mineral composition of clays in the subsurface layer of a clay blanket changes. As the pH of the solution being in contact with clays increases, the composition of the clay fraction changes by the simplified scheme: opal + alunite → opal + alunite + kaolinite → opal + kaolinite → opal + kaolinite + smectite → opal + smectite. The composition of the newly formed ore fraction depends significantly on E_h , which is expressed by the following sequence of transformations: marcasite + pyrite (pH ~ 3.5) → pyrite → hydrated hematite (limonite).

An assemblage of newly formed kaolinite, opal, and quartz forms in mud water pools with a weakly acidic medium (pH = 2–3); the ore fraction includes hematite and goethite. When the pH of the solution increases to 3.5, marcasite and pyrite appear in the ore fraction (marcasite can be present in significant amounts); with a subsequent increase in pH, marcasite disappears.

In mud water pools with a medium close to the neutral one, the clay fraction is newly formed smectite, whereas kaolinite is rare and occurs as an impurity. Also, opal and quartz can be present; pyrite prevails in the ore fraction. Alunite group minerals are absent. When such a pool dries out, the content of smectite decreases, the content of kaolinite increases, and a small amount of alunite group minerals might appear.

The channels of steam–gas jets are composed of kaolinite–montmorillonite assemblage, with the contents of kaolinite and alunite group minerals tending to increase. The content of marcasite increases in the ore fraction; sometimes, goethite is present.

In steaming ground, clays contain predominantly kaolinite, often better crystallized than that in mud water pools. Alunite group minerals are also present in significant amounts; the most common ones are natroalunite, ammoniojarosite, ammonioalunite, and minamiite (natroalunite-2R). The ore fraction contains goethite. The steaming ground is composed of the following mineral assemblages: opal + alunite group minerals + kaolinite + goethite and kaolinite + smectite + pyrite ± marcasite.

This work was supported by research project 0282-2016-0001 and grants 16-05-00007 and 18-35-00138 from the Russian Foundation for Basic Research.

REFERENCES

- Belousov, V.I., Lomonosov, I.S. (Eds.), 1993. The Structure of a Hydrothermal System [in Russian]. Nauka, Moscow.
- Chashchin, A.A., Martynov, Yu.A., Perepelov, A.B., Ekimova, N.I., Vladimirova, T.P., 2011. Physical and chemical conditions of the formation and evolution of Late Pleistocene–Holocene magmas of the Gorely and Mutnovsky Volcanoes, Southern Kamchatka. *Russ. J. Pacific Geol.* 5 (4), 348–367.
- Chukhrov, F.V. (Ed.), 1992. Minerals. Vol. 4. Issue 2. Layered Silicates [in Russian]. Nauka, Minerals.
- Drits, V.A., Ivanovskaya, T.A., Sakharov, B.A., Zviagina, B.B., Gorkova, N.V., Pokrovskaya, E.V., Savichev, A.T., 2011. Mixed-layer corrensite–chlorites and their formation mechanism in the glauconitic sandstone–clayey rocks (Riphean, Anabar uplift). *Lithol. Mineral. Res.* 46 (6), 566–593.
- Drits, V.A., Sakharov, B.A., Ivanovskaya, T.A., Pokrovskaya, E.V., 2013. Crystal-chemical microheterogeneity of Precambrian globular dioctahedral mica minerals. *Lithol. Mineral. Res.* 48 (6), 489–513.
- Eroshchev-Shak, V.A., Zolotarev, B.P., Karpov, G.A., 2005. Clay minerals in present-day volcano-hydrothermal systems. *J. Volcan. Seismol.*, No. 4, 11–21.
- Feofilaktov, S.O., Rychagov, S.N., Bukatov, Yu.Yu., Nuzhdaev, I.A., Nuzhdaev, A.A., 2017. New evidence relating to the structure of the zone of hydrothermal discharges in the East Pauzhetka thermal field, Kamchatka. *J. Volcan. Seismol.* 11 (5), 353–366.
- Frolova, Y.V., Ladygin, V.M., Luchko, M.V., Chernov, M.S., Rychagov, S.N., Boikova, I.A., 2016. Variation in the physical and mechanical properties of rocks: the North Paramushir hydrothermal magmatic system, Kuril Islands. *J. Volcan. Seismol.* 10 (3), 170–187.
- Geptner, A.R., Ivanovskaya, T.A., Pokrovskaya, E.V., Lyapunov, S.M., Savichev, A.T., Gorbunov, A.V., Gor'kova, N.V., 2007. Hydrothermally altered hyaloclastites at the Earth's surface in the rift zone of Iceland: problem of the biochemogenic accumulation of trace elements. *Lithol. Mineral. Res.* 42 (5), 453–476.
- Kalacheva, E.G., Rychagov, S.N., Koroleva, G.P., Nuzhdaev, A.A., 2016. The geochemistry of steam hydrothermal occurrences in the Koshelev volcanic massif, southern Kamchatka. *J. Volcan. Seismol.* 10 (3), 188–202.
- Kotenko, T.A., Kotenko, L.V., Sandimirova, E.I., Shapar', V.N., Timofeeva, I.F., 2012. The eruptive activity of the Ebeko Volcano (Paramushir Island) in 2010–2011. *Vestnik KRAUNTS. Nauki o Zemle*, No. 1, Issue 19, 160–167.
- Kravchenko, O.B., Rychagov, S.N., 2017. The structure and lithogenesis of hydrothermal clay strata of the Lower Koshelevskii geothermal anomaly (southern Kamchatka). *Litosfera*, No. 2, 95–114.
- Krupskaya, V.V., Miroshnikov, A.Y., Dorzhieva, O.V., Zakusin, S.V., Semenov, I.N., Usacheva, A.A., 2017. Mineral composition of soils and bottom sediments in bays of Novaya Zemlya. *Oceanology* 57 (1), 215–221.
- Ladygin, V.M., Frolova, Y.V., Rychagov, S.N., 2014. The alteration of effusive rocks due to acidic leaching by shallow thermal waters: the Baranskii geothermal system, Iturup Island. *J. Volcanol. Seismol.* 8 (1), 17–33.
- Madejova, J., 2003. FTIR techniques in clay mineral studies. *Vib. Spectrosc.* 31, 1–10.
- Madejova, J., Komadel, P., 2001. Baseline studies of the Clay Minerals Society source clays: infrared methods. *Clays Clay Miner.* 49, 410–432.
- Martinez, J.C., Dristas, J., Massonne, H.-J., Theye, T., 2006. Alunite and REE rich APS minerals associated to the hydrothermal clay deposits in the Barker Area, Tandilia, Argentina. *Clay Sci.*, No. 12, Suppl. 2, 15–20.
- Masurenkov, Yu.P., 1980. The Long-Living Center of Endogenic Activity of Southern Kamchatka [in Russian]. Nauka, Moscow.
- Miyoshi, Y., Ishibashi, J.-I., Shimada, K., Inoue, H., Uehara, S., Tsukimura, K., 2015. Minerals in an active hydrothermal field at Iheya-North-Knoll, Okinawa Trough. *Resour. Geol.* 65 (4), 346–360.
- Murowchick, J.B., Barnes, H.L., 1986. Marcasite precipitation from hydrothermal solutions. *Geochim. Cosmochim. Acta* 50, 2615–2629.
- Ogorodova, L.P., Kiseleva, I.A., Melchakova, L.V., Krupskaya, V.V., Vigasina, M.F., 2013. Thermochemical study of natural montmorillonite. *Geochem. Int.* 51 (6), 484–494.
- Pamela, J.M., Adrian, M.L.S., Karen, A.H.-E., William, E.D., Kate, W., 2009. Raman and IR spectroscopic studies of alunite-supergroup compounds containing Al, Cr³⁺, Fe³⁺ and V³⁺ at the B site. *Can. Mineral.* 47, 663–681.
- Pozdeev, A.I., Nazhalova, I.N., 2008. The geology, hydrodynamics, and the oil and gas potential of the Kosheleva stream–water field in Kamchatka. *J. Volcan. Seismol.* 2 (3), 170–183.
- Rychagov, S.N., 2014. Giant gas-rich hydrothermal systems and their role in the generation of vapor-dominated geothermal fields and ore mineralization. *J. Volcan. Seismol.* 8 (2), 69–92.
- Rychagov, S.N., Koroleva, G.P., Stepanov, I.I., 2002. Ore elements in the hypergenesis zone of a steam hydrotherm deposit: distribution, migration forms, and sources. *J. Volcan. Seismol.*, No. 2, 37–58.
- Rychagov, S.N., Davletbaev, R.G., Kovina, O.V., Koroleva, G.P., 2008. Characteristics of the subsurface horizon of hydrothermal clays of the Lower Koshelevskii and Pauzhetka hydrothermal deposits. *Vestnik KRAUNTS. Nauki o Zemle*, No. 2, Issue 12, 116–134.
- Rychagov, S.N., Davletbaev, R.G., Kovina, O.V., 2009a. Hydrothermal clays and pyrite in geothermal fields: their significance for the geochemistry of present-day endogenous processes in Southern Kamchatka. *J. Volcan. Seismol.* 3 (2), 105–120.
- Rychagov, S.N., Nuzhdaev, A.A., Stepanov, I.I., 2009b. Behavior of mercury in the supergene zone of geothermal deposits, Southern Kamchatka. *Geochem. Int.* 47 (5), 504–512.
- Rychagov, S.N., Sokolov, V.N., Chernov, M.S., 2010. Hydrothermal clays as a highly dynamical colloid-disperse mineralogical-geochemical system. *Dokl. Earth Sci.* 435 (2), 1684–1687.
- Rychagov, S.N., Davletbaev, R.G., Kovina, O.V., Sergeeva, A.V., Sokolov, V.N., Chernov, M.S., Shchegolkov, Y.V., 2012a. Cation migration in hydrothermal clays: the problem of mineralization criteria in gas-hydrothermal fluids of hydrothermal fields in Southern Kamchatka. *J. Volcan. Seismol.* 6 (4), 230–242.
- Rychagov, S.N., Sokolov, V.N., Chernov, M.S., 2012b. Hydrothermal clays of the geothermal fields of South Kamchatka: a new approach and study results. *Geochem. Int.* 50 (4), 344–357.
- Rychagov, S.N., Nuzhdaev, A.A., Stepanov, I.I., 2014. Mercury as an indicator of modern ore-forming gas-hydrothermal systems, Kamchatka. *Geochem. Int.* 52 (2), 131–143.
- Rychagov, S.N., Sandimirova, E.I., Sergeeva, A.V., Nuzhdaev, I.I., 2017a. Composition of the ash of the Kambal'nyi Volcano (erupted in 2017). *Vestnik KRAUNTS. Nauki o Zemle*, No. 4, Issue 36, 13–27.

- Rychagov, S.N., Sergeeva, A.V., Chernov, M.S., 2017b. Mineral Assemblages of the clay stratum basement as indicators of the fluid regime of the Pauzhetka hydrothermal system (Kamchatka). *Tikhookeanskaya Geologiya* 36 (6), 90–106.
- Rychagov, S.N., Sergeeva, A.V., Chernov, M.S., 2017c. Specific mineral associations of hydrothermal shale (South Kamchatka). *Dokl. Earth Sci.* 477 (1), 1301–1306.
- Vasilevskii, M.M., 1977. Predictive Assessment of the Ore Potential of Volcanic Rock Associations [in Russian]. Nedra, Moscow.
- Zhitova, E.S., Siidra, O.I., Shilovskikh, V.V., Belakovsky, D.I., Nuzhdaev, A.A., Ismagilova, R.M., 2017. Ammoniovoltaite, IMA 2017-022. *CNMNC Newsletter* No. 38, August 2017. *Miner. Mag.* 81, 1033–1038.
- Zhitova, E.S., Siidra, O.I., Belakovsky, D.I., Shilovskikh, V.V., Nuzhdaev, A.A., Ismagilova, R.M., 2018. Ammoniovoltaite, $(\text{NH}_4)_2\text{Fe}_5^{2+}\text{Fe}_3^{3+}\text{Al}(\text{SO}_4)_{12}(\text{H}_2\text{O})_{18}$, a new mineral from the Severo-Kambalny geothermal field, Kamchatka, Russia. *Miner. Mag.* 82 (5), 1057–1077. doi: 10.1180/minmag.2017.081.083.

Editorial responsibility: N.L. Dobretsov